Meteorin-like/meteorin-β protects against cardiac dysfunction after myocardial infarction in mice by inhibiting autophagy

JIAHONG SHANGGUAN, GANGQIONG LIU, LILI XIAO, WENJING ZHANG, XIAODAN ZHU and LING LI

Department of Cardiology, The First Affiliated Hospital of Zhengzhou University, Zhengzhou, Henan 450052, P.R. China

Abstract. Meteorin-β (Metrnβ) is a protein that is secreted by skeletal muscle and adipose tissue, and participates in cardiovascular diseases. However, its role in myocardial infarction (MI) has not been fully elucidated to date. The aim of the present study was to investigate the role and underlying mechanism of Metrnβ in MI. In the present study, mice were subjected to left coronary ligation to induce a MI model before being injected with adeno-associated virus 9 (AAV9)-Metrnβ to overexpress Metrnβ. Mice were subjected to echocardiography and pressure-volume measurements 2 weeks after ligation. Cardiac injury was measured from the levels of cardiac troponin T and pro-inflammatory factors, which were detected using ELISA kits. Cardiac remodelling was determined from the cross-sectional areas detected using H&E and wheat germ agglutinin staining as well as from the transcriptional levels of hypertrophic and fibrosis markers detected using reverse transcription-quantitative PCR. Cardiac function was detected using echocardiography and pressure-volume measurements. In addition, H9c2 cardiomyocytes were transfected with Ad-Metrnβ to overexpress Metrnβ, before being exposed to hypoxia to induce ischaemic injury. Apoptosis was determined using TUNEL staining and caspase 3 activity. Cell inflammation was detected using ELISA assays for pro-inflammatory factors. Autophagy was detected using LC3 staining and assessing the protein level of LC3II using western blotting. H9c2 cells were also treated with rapamycin to induce autophagy. It was revealed that Metrnβ expression was reduced in both mouse serum and heart tissue 2 weeks post-MI. Metrnβ overexpression using AAV9-Metrnβ delivery reduced the mortality rate, decreased the infarction size and reduced the extent of myocardial injury 2 weeks post-MI. Furthermore, Metrnβ overexpression inhibited cardiac hypertrophy, fibrosis and inflammation post-MI. In ischaemic H9c2 cells, Metrnβ overexpression using adenovirus also reduced cell injury, cell death and inflammatory response. Metrnβ overexpression suppressed MI-induced autophagy *in vitro*. Following autophagy activation using rapamycin *in vitro*, the protective effects induced by Metrnβ were reversed. Taken together, these results indicated that Metrnβ could protect against cardiac dysfunction post-MI in mice by inhibiting autophagy.

Introduction

Myocardial infarction (MI), which is predominantly caused by myocardial ischaemia, leads to large areas of myocardial cell necrosis and apoptosis (1). Cardiac remodelling after MI is characterized by inflammation, fibrosis and cardiac hypertrophy in the remaining myocardium (2). This adverse cardiac remodelling eventually leads to heart failure (3,4). To date, although emergency coronary artery revascularization can save the life of patients with acute MI (AMI) and numerous anti-heart failure treatments (such as angiotensin receptor antagonists and β adrenergic receptor blockers) designed to suppress adverse cardiac remodelling exist, the incidence of heart failure (with an estimated prevalence of >37.7 million individuals globally) and mortality caused by AMI remains high at an incidence of ~10% worldwide (4,5). Therefore, there is a demand to identify novel effective treatment strategies for MI and MI-induced heart failure.

Autophagy is an important process of energy metabolism. Under conditions of energy deprivation, autophagy is activated, which degrades intracellular organelles and proteins into amino acids and fatty acids to produce energy substrates for the recycling of energy (6). Basal levels of autophagy are essential for the maintenance of cardiac function. Autophagy is activated to protect cardiomyocytes from ischaemia or ischaemia/reperfusion injury under conditions of short-term myocardial ischaemia stress (7). However, under chronic myocardial hypoxia, excessive activation of autophagy aggravates necrosis and apoptosis in myocardial cells, which in turn accelerates the adverse progression of myocardial remodelling (7). Therefore, investigation into the modulation of autophagy activation is an important topic for slowing the progression of myocardial remodelling after MI to prevent heart failure.

Meteorin-β (Metrnβ), which is also known as interleukin (IL)-41, is a secretory protein that is mainly secreted by skeletal muscle and adipose tissue (8). Previous studies have

---

Correspondence to: Dr Ling Li, Department of Cardiology, The First Affiliated Hospital of Zhengzhou University, 1 Jianshe East Road, Zhengzhou, Henan 450052, P.R. China
E-mail: liling_63035@126.com

revealed that it likely regulates energy metabolism in skeletal muscle and adipose tissues (9,10). However, other studies have revealed that Metrnβ is closely associated with immunity, inflammation, obesity and diabetes (9,10). In addition, recent studies have reported that Metrnβ serves a role in cardiovascular diseases (11,12). Following isoproterenol stimulation, Metrnβ-knockout mice exhibited myocardial hypertrophy, fibrosis and heart failure. However, Metrnβ overexpression could inhibit this type of myocardial remodelling induced by isoproterenol (11). In addition, another study reported that myocardial cells could also secrete Metrnβ, and that the concentration of Metrnβ in the human serum was correlated (Pearson correlation) with the prognosis of heart failure (12). However, the role of Metrnβ in MI remains to be fully elucidated. Therefore, the present study aimed to explore the role and underlying mechanism of Metrnβ in MI. In the present study, the effects and the underlying mechanism of Metrnβ on MI-induced cardiac remodelling were explored.

Materials and methods

Animals. C57BL6J male 8-week-old mice (24-27 g) were purchased from Beijing Huafukang Biotechnology Co., Ltd. The animals were housed with a maximum of six other mice in individually-ventilated cages (with a floor area of 542 cm^2 and bedded with corncob). The animals were allowed free access to food and water and were maintained on a 12 h light/dark cycle in a controlled temperature (20-25℃), humidity (50±5%) and specific pathogen-free environment (13). In total, 90 mice were used, among which 16 mice (n=6 for the sham group; n=10 for the MI group) were used to detect alterations in the Metrnβ expression levels after being subjected to MI. The other 74 mice were divided into four groups: Adeno-associated virus 9 (AAV9)-negative control (NC)-sham group (n=12); AAV9-Metrnβ-sham group (n=12); AAV9-NC-MI group (n=25); and AAV9-Metrnβ-MI group (n=25). Mice in the MI groups were subjected to left anterior descending (LAD) coronary artery ligation surgery. For AAV9 injection, mice were subjected to retro-orbital venous plexus injection of either AAV9-NC or AAV9-Metrnβ 2 weeks before surgery. Animal health and behaviour were monitored daily. Being incapable of maintaining normal activities (n=3, after MI surgery) or eating on their own (n=1) were the humane endpoints used to determine when the animals should be sacrificed to minimize suffering. During and after the ligation operation, 26 mice died from MI. The remaining 60 mice were sacrificed at the end of the scheduled experiment to collect the heart tissue. Mice were euthanized by cervical dislocation under anaesthesia (2% isoflurane) and mortality was verified by the cessation of breathing and heartbeat. The animal experiments were performed (Sep. 2021 to Dec. 2022) according to the Animal Research: Reporting of *in vivo* Experiments guidelines (14) and were approved by the Animal Care and Use Committee of the First Affiliated Hospital of Zhengzhou University (approval no. 2021-02623).

Animal model of MI. LAD was conducted according to a previously published protocol (15). Briefly, anaesthesia was induced in mice by 2% isoflurane and maintained with 1.5% isoflurane through a face mask, before the mice were placed in a supine position. The thorax between the left third and fourth ribs was then opened. After the pericardium was excised, 7-0 threads were ligated at the proximal end of the left coronary artery. For the sham operation, all of the procedures were the same except ligation. After surgery, buprenorphine (0.1 mg/kg, subcutaneously injected) was used for postoperative analgesia in mice. The success of the MI was evaluated by the increased cardiac troponin T (cTnT) levels in the blood samples 12 h after LAD (three times that of the sham group). When sampling the heart tissues, the atrium was first removed to expose the ventricular cavities before the thinner right ventricular tissues were removed to collect the left ventricular tissues.

AAV9-Metrnβ and the control AAV9-NC construction and viral delivery. AAV9-Metrnβ and the AAV9-NC [also AAV9-green fluorescent protein (AAV9-GFP)], both with TnT promoters, were purchased from the Vigene Bioscience Company. The plasmids pCI-Metrnβ-his6 and an empty vector (pCI-NC) were used for AAV9-Metrnβ and AAV9-NC, respectively. Mice were randomly assigned to receive either 60-80 μl AAV9-Metrnβ or AAV9-NC at 5.0-6.5x10^{13} gene copy/ml in sterile PBS at 37℃ by injection into the retro-orbital venous plexus 2 weeks before LAD surgery, as described in a previous study (14). Briefly, 2% isoflurane was used to induce and maintain anaesthesia in mice and a drop of ophthalmic anaesthetic (0.5% proparacaine hydrochloride ophthalmic solution) was placed on the eye that received the injection.

Echocardiography measurements. Echocardiography was conducted according to previously published guidance (15). Mice were anesthetized with 1.5-2.0% isoflurane to induce and maintain anaesthesia. Echocardiography with a Mylab 30CV (Esaote) was used to measure cardiac function 2 weeks post MI. The M Doppler uses a 15-mHz probe to detect and record cardiac function. The left ventricular (LV) ejection fraction (LVEF) and LV fractional shortening (LVFS) were calculated after data collection. The software MyLab™ Desk version 3 (Esaote) was used to calculate HR and LVEF. LVFS was calculated using the following formula:

LVFS (%)=(LVEDd-LVESd) x(100%/LVEDd); LVEF (%)=(LVEDd^3-LVESd^3) x(100%/LVEDd^3). After echocardiography, mice were then subjected to haemodynamic detection.

Pressure-volume measurements. Haemodynamic detection was conducted according to a previous study 2 weeks post MI (16). Anaesthesia in mice was induced with 2% isoflurane and maintained with 1.5% isoflurane (17,18). A 1.4 French (4.5 mm) Millar catheter transducer (Millar, Inc.) was transferred from the right carotid artery in the right of the neck to the left ventricle. A Millar pressure-volume system (MPVS-400; Millar, Inc.) and a Powerlab/4SP A/D converter (AD instruments, Inc.) were used to continuously record the pressure signals and heart rate. Heart rate, end systolic volume, end diastolic volume, maximal rate of systolic pressure increment (+dp/dt) and diastolic pressure decrement (-dp/dt) and cardiac output were calculated and corrected according to *in vitro* and *in vivo* volume calibrations with PVAN 2.3 software (ADInstruments, Ltd.). The hearts were collected after haemodynamic detection.

H&E and picrosirius red (PSR) staining. H&E and PSR staining were conducted according to previously published guidance (19,20). Briefly, heart sections (4-5 μm thick) were prepared, and sections stained with H&E were separated by 500 μm to determine infarct size. Image-Pro Plus, version 6.0 (Media Cybernetics, Inc.), was used to calculate MI size. Cross-sectional areas of cardiomyocytes were observed using FITC-combined wheat germ agglutinin (WGA) and cTnT (Invitrogen; Thermo Fisher Scientific, Inc.) fluorescence staining. The nuclei were stained with 4',6-diamino-2-phenylindole (DAPI). Image-Pro Plus (version 6.0) was used to measure the myocardial cell cross-sectional area.

Several sections of each heart (4-5-mm thick) were prepared and stained with PSR for collagen deposition analysis, and they were then visualized with light microscopy. The LV collagen volume fraction was calculated from the PSR-stained sections as the area stained by PSR divided by the total area. Image-Pro Plus (version 6.0) was used to measure the myocardial cell cross-sectional area and LV collagen fraction.

Enzyme-linked immunosorbent assay (ELISA) detection of inflammatory cytokines. Heart tissue samples and cell samples were lysed and tested using ELISA. The inflammatory cytokine indicators included tumour necrosis factor α (TNFα; LEGEND MAX™ Mouse TNF-α ELISA kit; cat. no. #430907), IL-1β (ELISA MAX™ Deluxe Set Mouse IL-1α; cat. no. #433404) and IL-6 (LEGEND MAX™ Mouse IL-6 ELISA kit; cat. no. #431307). The aforementioned ELISA kits were purchased from BioLegend, Inc. The ELISA kit for Metrnβ (Mouse Meteorin-like/METRNL DuoSet ELISA; cat. no. DY6679) was purchased from R&D Systems China Co., Ltd. The concentration of each sample was calculated using the standard curve method.

cTnT levels in blood samples. The venous blood from tail vein (100-200 μl) of mice was collected 12 h after the LAD operation, and serum cTnT concentrations were detected after 200 x g centrifugation for 15 min at 4˚C. All steps were performed according to the manufacturer's protocols of the cardiac troponin assay kit (cat. no. #H149-4-1; Nanjing Jiancheng Bioengineering Institute). The ELISA plate reader (Synergy HT; Agilent Technologies, Inc.) was used for detection.

Cell culture. H9c2 rat cardiomyocytes were purchased from The Cell Bank of Type Culture Collection of The Chinese Academy of Sciences. Dulbecco's minimum essential medium (DMEM) (cat. no. C11995; Gibco; Thermo Fisher Scientific, Inc.) supplemented with 10% foetal bovine serum (FBS; Thermo Fisher Scientific, Inc.) was used for cell culture at 37˚C (95% O_2 and 5% CO_2) (21,22). A cell hypoxia model was induced for 24 h at 37˚C by culturing with 5% O_2, 5% CO_2 and 90% nitrogen. Control cells were cultured in a normal atmosphere at 37˚C, 5% CO_2 and 95% air (21% O_2 and 78% nitrogen).

Transfection and treatments. After culture with FBS-free DMEM for 12 h at 37˚C, cells were transfected with adenovirus overexpress with Metrnβ (Ad-Metrnβ; MOI=50; diluted with PBS) for 24 h at 37˚C to overexpress Metrnβ. Adenovirus

carrying a control vector (Ad-NC; MOI=50) was used as control (pAd-CMV-V5 vector; Invitrogen; Thermo Fisher Scientific, Inc.). To silence Metrnβ expression, cells were transfected with the small interfering RNA (siRNA) against Metrnβ (Metrnβ siRNA; 50 nM; Guangzhou RiboBio Co., Ltd.) for 24 h at 37˚C using the Lipo 6000™ transfection reagent (Beyotime Institute of Biotechnology). A scramble siRNA (scRNA) was used as control. The transfected sequences used were as follows: Metrnβ siRNA (sense 5'-CACGCTTTAGTGACTTTCAAA-3' and antisense 5'-TTTGAAAGTCACTAAAGCGTG-3'); and scRNA (sense 5'-TTCTCCGAACGTGTCACGT-3' and antisense 5'-ACGTGACACGTTCGGAGAA-3'). Cells were used for subsequent functional experiments at 24 h post-transfection.

In addition, cells were treated with bafilomycin A1 (BAF; 100 nM; MedChemExpress) or rapamycin (10 mM; MedChemExpress) for 12 h at 37˚C to block autophagosome degradation or activate autophagy, respectively, before being transfected with Ad-Metrnβ for 24 h.

Cell Counting Kit-8 (CCK-8) assay. H9c2 cell viability was detected using the CCK-8 Kit (cat. no. HY-K0301; MedChemExpress) according to the manufacturer's protocols. Briefly, the cell density was adjusted to 1x10^5/ml and 96-well plates were used for cell culture (overnight at 37˚C with 95% O_2 and 5% CO_2). In total, 10 μl CCK-8 solution was added to each well and then cultured for another 3 h at 37˚C. An ELISA plate reader (Synergy HT; BioTek Instruments, Inc.) was used to determine the absorbance at 450 nm. Each group has triplicates.

Western blotting. H9c2 cells and heart tissues were lysed in radioimmunoprecipitation (RIPA) lysis buffer [720 μl RIPA; 20 μl PMSF (1 mM); 100 μl cOmplete (cat. no. 04693124001; Roche Diagnostics); 100 μl PhosSTOP (cat. no. 04906837001; Roche Diagnostics); 50 μl NaF (1 mM); 10 μl Na$_3$VO$_4$; per ml]. Protein concentrations of the heart tissues and cells were determined using the BCA Protein Detection kit (Beyotime Institute of Biotechnology). Total protein was isolated using 4-12% gels and sodium dodecyl sulphate polyacrylamide gel electrophoresis (50 μg/sample) and transferred to polyvinylidene difluoride membranes (Merck KGaA). Following blocking with 5% skimmed milk powder for 2 h at room temperature, the membranes were then incubated with primary antibodies (all from Cell Signaling Technology, Inc.) against LC3 (cat. no. #2775; 1:1,000), p62 (cat. no. #23214; 1:1,000) or GAPDH (cat. no. #2118; 1:1,000) at 4˚C overnight. The membranes were then incubated with the HRP-conjugated goat anti-rabbit IgG secondary antibody (cat. no. ab6721; 1:2,000; Abcam) for 1 h at room temperature. Protein band visualization was performed using Clarity™ Western ECL Substrate (cat. no. #1705060; Bio-Rad Laboratories, Inc.). ChemiDoc MP imaging system (Bio-Rad Laboratories, Inc.) was used for imaging. Band intensities were semi-quantified using ImageJ software (v1.8.0.112; National Institutes of Health).

Reverse transcription-quantitative PCR. Total mRNA from the left ventricle of the heart tissues was extracted from frozen, pulverized mouse cardiac tissue using TRIzol™ (cat. no. 15596-026; Thermo Fisher Scientific, Inc.). cDNA

was synthesized using a reverse transcription kit (Roche Diagnostic) at 70°C for 5 min. The LightCycler® 480 SYBR Green I kit (Roche Diagnostics) was used for amplification. Following an initial 5 min denaturation step at 95°C, a total of 42 primer-extension cycles were carried out. Each cycle consisted of a 10 sec denaturation step at 95°C, a 20 sec annealing step at 60°C and a 20 sec incubation at 72°C for extension. Subsequently, a final extension step was performed at 72°C for 10 min. The relative expression level of indicated genes was compared with that of GAPDH expression fold changes. The $2^{-\Delta\Delta Cq}$ method was used for quantification (14). The primers used are listed in Table I.

Metrnβ concentration detection. Serum and heart tissue samples were first collected. Heart tissues were lysed in RIPA lysis buffer before centrifugation. After centrifugation with 900 x g for 15 min at 4°C, an ELISA kit for Metrnβ (Mouse Meteorin-like/METRNL DuoSet ELISA; cat. no. DY6679) was purchased from R&D Systems China Co., Ltd., and an ELISA plate reader were used for detection.

Lactate dehydrogenase (LDH) release and caspase-3 activity. After hypoxia or control treatments, the cell culture medium was collected and centrifuged (100 x g for 10 min at 4°C) and the LDH detection kit (cat. no. A020-2-2; Nanjing Jiancheng Bioengineering Institute) was used to detect LDH level.

Caspase-3 activity was evaluated using the Caspase-3 Activity Assay kit (cat. no. #5723; Cell Signaling Technology, Inc.) after washing. An ELISA plate reader was used for detecting fluorescence at 380 nm excitation and at 450 nm emission. Caspase-3 activity was calculated as fluorometric signal excitation/emission=380/450 nm and as the fold-change to the control group.

TUNEL staining. TUNEL staining was performed as described in our previous study (23). Briefly, after the cells were fixed with RCL2® (cat. no. RCL2-CS24L; ALPHELYS) at room temperature for 5 min, TUNEL staining was performed using the Apo-Direct TUNEL Assay kit (cat. no. APT110; MilliporeSigma) for 1 h at room temperature. The cells on coverslips were mounted onto glass slides with culture media. The nuclei were labelled with 0.29 μM DAPI at room temperature for 5 min, and the percentage of TUNEL-positive cells was calculated using microscopy. The outline of 40 cells from each group were visualized by fluorescence microscopy (BX51TRF; Olympus Corporation). For each slide 10 fields of view were observed.

Immunofluorescence staining and autophagic flux analysis. Cells were fixed with 0.2% RCL2® (cat. no. RCL2-CS24L; ALPHELYS) at room temperature for 5 min, immobilized, sealed with 10% goat serum (Absin Bioscience, Inc.) at room temperature for 30 min, and incubated overnight at 37°C with antibody against LC3 (cat. no. 2775; 1:500; Cell Signaling Technology, Inc.). The cells were then incubated with Alexa Fluor™ 488 goat anti-rabbit IgG (cat. no. A31627; 1:10,000; Invitrogen; Thermo Fisher Scientific, Inc.) secondary antibody for 1 h at 37°C. The nuclei were stained with 0.29 μM DAPI at room temperature for 5 min. Images were captured using an Olympus DX51 fluorescence microscope (Olympus

Corporation). Image Pro Plus (version 6.0) was used to quantify fluorescence intensity.

To detect changes in autophagic flow, cells were infected with monomeric red fluorescent protein (mRFP)-GFP-LC3 adenovirus (Ad-mRFP-GFP-LC3; MOI, 100) for 8 h at 37°C before 24 h of hypoxic culturing. The number of red and green puncta in the cells was counted (10 fields of view/dish) after images were captured with a fluorescence microscope.

Adult mouse cardiomyocyte/cardiac macrophage isolation. Adult mouse cardiomyocytes were obtained from mice 2 weeks post-MI using the Langendorff method according to a previous study (24). The mouse hearts were removed and attached to the Langendorff perfusion system (Radnoti; ADInstruments, Ltd.) in 1x basal solution with 10 mM d-(+)-Glucose, 10 mM 2,3-butanedione monoxime and 5 mM taurine. The pH was adjusted to 7.4 at 37°C and filtered with a bottle top filtration unit. The heart was then digested using a circulating enzyme digestion solution (collagenase type 2; CAS no. 9001-12-1; AbMole Bioscience Inc.; the pH was adjusted to 7.4 at 37°C with a final concentration of 525 U/ml) at 37°C for 15-20 min. The physiological morphology of cardiomyocytes was then observed though microscope, with a 'brick-like' appearance considered to be 'healthy'. The isolated cardiomyocytes were then filtered through a 250 μm filter and seeded onto culture dishes coated with 20 mM HEPEs, 4 mM NaHCO$_3$, 0.1 mg/ml bovine serum albumin (AbMole Bioscience Inc.) and 10 μg/ml laminin (Abcam) at 37°C for 12 h.

Adult mouse hearts were removed from mice post-MI and digested with 100 μg/ml collagenase II at 37°C for 30 min a total of five times (25). The cells were then filtered through a 250 μm filter and re-suspended in culture medium. Non-specific binding was blocked with TruStain FcX antibody (cat. no. 101320; 1:1,000; BioLegend, Inc.) at 37°C for 15 min. The macrophages (10^6) were then washed with 10 ml FACS buffer and labelled with the following antibodies (all from BioLegend, Inc.): CD45-PerCPCy5.5 (2 μg/ml) and F4/80-PE (6 μg/ml) The macrophages were sorted using flow cytometry (Fig. S1) (BD FACSCanto II flow cytometer; BD Biosciences).

Statistical analysis. All data are expressed as the mean ± standard deviation. All data were normally distributed, which was confirmed by the Shapiro-Wilk test. The differences between two groups were analysed using an unpaired Student's t-test. One-way ANOVA analysis followed by Tukey's post hoc test was used to compare the four groups, whereas two-way ANOVA analysis followed by Tukey's post hoc test was used to compare the four/six groups with two variables. P<0.05 was considered to indicate a statistically significant difference. Each experiment was repeated three times for the *in vitro* H9c2 experiments.

Results

Metrnβ is downregulated upon MI in mice. The levels of Metrnβ were detected in mice that were subjected to MI. There was no difference in the HRs between the sham and MI groups within the experimental series (Table II). The results indicated that Metrnβ expression levels were significantly reduced in the plasma (1887±284 vs. 630±252 pg/ml; P<0.01,

Table I. Primer sequences used for reverse transcriptase-quantitative PCR.

mRNA	Forward (5'-3')	Reverse (5'-3')
ANP	ACCTGCTAGACCACCTGGAG	CCTTGGCTGTTATCTTCGGTACCGG
BNP	GTCAGTCGTTTGGGCTGTAAC	AGACCCAGGCAGAGTCAGAA
Collagen I	AGGCTTCAGTGGTTTGGATG	CACCAACAGCACCATCGTTA
Collagen III	AAGGCTGCAAGATGGATGCT	GTGCTTACGTGGGACAGTCA
α-SMA	AACACGGCATCATCACCAAC	ACCAGTTGTACGTCCAGAGG
GAPDH	ACTCCACTCACGGCAAATTC	TCTCCATGGTGGTGAAGACA

ANP, atrial natriuretic peptide; BNP, B-type natriuretic peptide; α-SMA, α-smooth muscle actin.

Table II. Heart rate of mice used for detection of Meteorin-β protein expression levels.

Experimental series	Sham (bpm)	MI (bpm)
Mice for collecting heart tissue	482±7	480±10
Mice for collecting cardiomyocytes	476±12	468±14
Mice for collecting macrophages	465±9	478±12

Heart rate of mice used for detection of Meteorin-β protein expression levels in heart tissues, isolated cardiomyocytes and isolated macrophage. There was no difference in heart rate between groups within the experimental series. bpm, beat per minute.

sham vs. MI, respectively) (Fig. 1A) and in the heart tissue (931±120 vs. 309±137 pg/ml; P<0.01, sham vs. MI, respectively) (Fig. 1B and C) of mice in response to MI stress. Metrnβ is reported as mainly secreted by macrophages (10). The expression levels of Metrnβ on cardiomyocytes isolated from MI heart tissue and the expression levels of Metrnβ on macrophages isolated from MI heart tissue were therefore detected in the present study. The Metrnβ levels in cardiomyocytes isolated from MI heart tissue were significantly decreased (Fig. 1D). The Metrnβ levels in macrophages demonstrated no significant difference when the MI samples were compared with the control samples (Figs. 1E and S1). Thus, these data suggested that the decreased Metrnβ levels were mainly due to reduced expression in the cardiomyocytes.

Metrnβ overexpression improves cardiac parameters post MI. To further investigate the role of Metrnβ in MI, Metrnβ was overexpressed using AAV9, which has been reported to target the heart, specifically cardiomyocytes (26). Mice were also subjected to LAD surgery 2 weeks after injection with AAV9 (Fig. 2A). Successful overexpression was confirmed by Metrnβ protein level measurements, and AAV9-Metrnβ increased the plasma Metrnβ levels by greater than two times compared with the AAV9-NC in the sham treatment group as well as in the MI treatment group (Fig. 2B). Additionally, the Metrnβ protein levels in the heart tissues were also increased in the AAV9-Metrnβ group compared with the AAV9-NC group in both the sham and MI treatment groups (Fig. 2C). Furthermore, 2 weeks after MI surgery, the level of Metrnβ in

cardiomyocytes isolated from mouse hearts was significantly increased in the two AAV9-Metrnβ groups compared with the two respective AAV9-NC groups (Fig. 2D). The cTnT levels were increased at 12 h post-MI in the two MI treatment groups, and there was no difference between AAV9-Metrnβ and AAV9-NC, which suggested MI occurred to the same extent in both of these MI groups (Fig. 2E). Metrnβ overexpression markedly increased the post-MI survival rate (Fig. 2F). The cell death parameters were examined, and Metrnβ overexpression significantly lowered the infarct size (Fig. 2G). Furthermore, hypotrophy parameters were investigated and revealed that Metrnβ overexpression inhibited the MI-induced increase in the cross-sectional area, as well as atrial natriuretic peptide (ANP) and B-type natriuretic peptide (BNP) gene transcription (Fig. 2H and I).

Metrnβ overexpression protects the heart from MI-induced fibrosis and inflammation. Cardiac fibrosis is a characteristic of adverse cardiac remodelling post MI that leads to heart failure (27). The LV collagen volume was detected using PSR staining. Mice in the MI group exhibited marked LV collagen deposits 2 weeks after MI, while Metrnβ overexpression reversed this effect (Fig. 3A and B). The levels of fibrotic markers were also reduced by Metrnβ overexpression compared with the levels in the mice that received the AAV9-NC (Fig. 3B). Inflammation is the initiating factor of cardiac fibrosis after MI (28). Proinflammatory factors were increased in the two MI groups 2 weeks after MI. Metrnβ overexpression reduced the increase in the levels of the proinflammatory factors, as shown in the comparison between the AAV9-Metrnβ group and the AAV9-NC group (Fig. 3C).

Metrnβ overexpression preserved cardiac function post MI. The progression of heart failure was revealed by heart weight (HW) and lung weight (LW). The HW/body weight (BW) ratio and the LW/BW ratio were increased in the two MI groups compared with those of the two sham groups at 2 weeks post-MI, which indicated adverse cardiac hypertrophy and lung oedema. Metrnβ overexpression reversed the cardiac hypertrophy and lung oedema observed in the AAV9-NC group (Fig. 4A). Cardiac function was also evaluated using echocardiography and pressure-volume measurements. All the groups demonstrated similar HR levels (Fig. 4B). The LV end diastolic diameter (LVEDD)
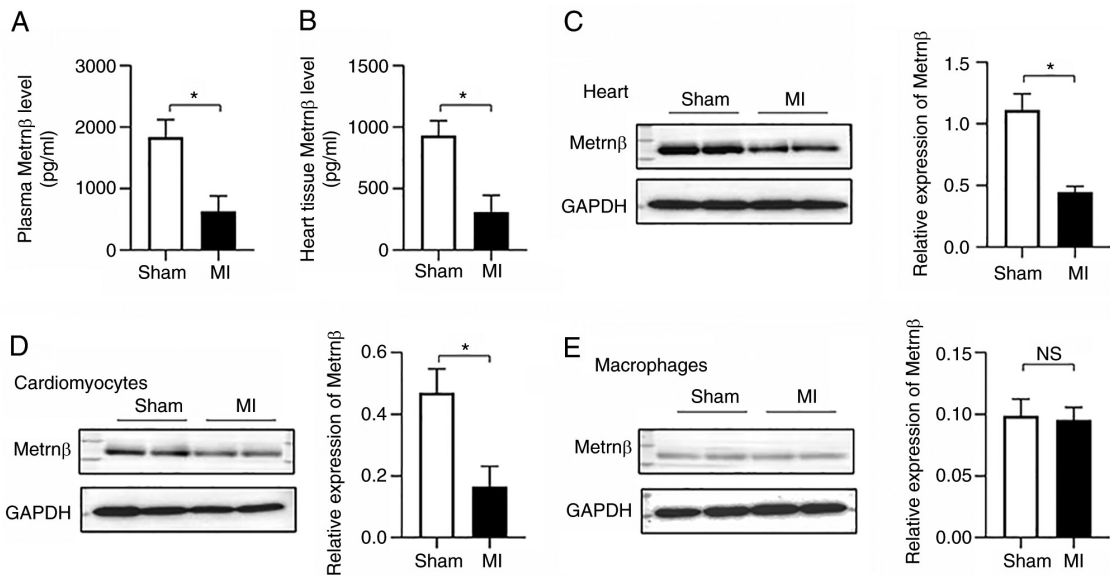
Figure 1. Metrnβ is downregulated upon MI in mice. (A) Plasma levels of Metrnβ in mice (n=6). (B) Levels of Metrnβ in mouse hearts (n=6). (C) Protein levels of Metrnβ in mice (n=4). (D) Protein levels of Metrnβ in cardiomyocytes isolated from adult mouse hearts (n=4). (E) Protein levels of Metrnβ in macrophages isolated from adult mouse hearts (n=4). *P<0.05. Student's t-test was used for the comparison between two groups. Metrnβ, meteorin-β; MI, myocardial infarction; NS, no significant difference.
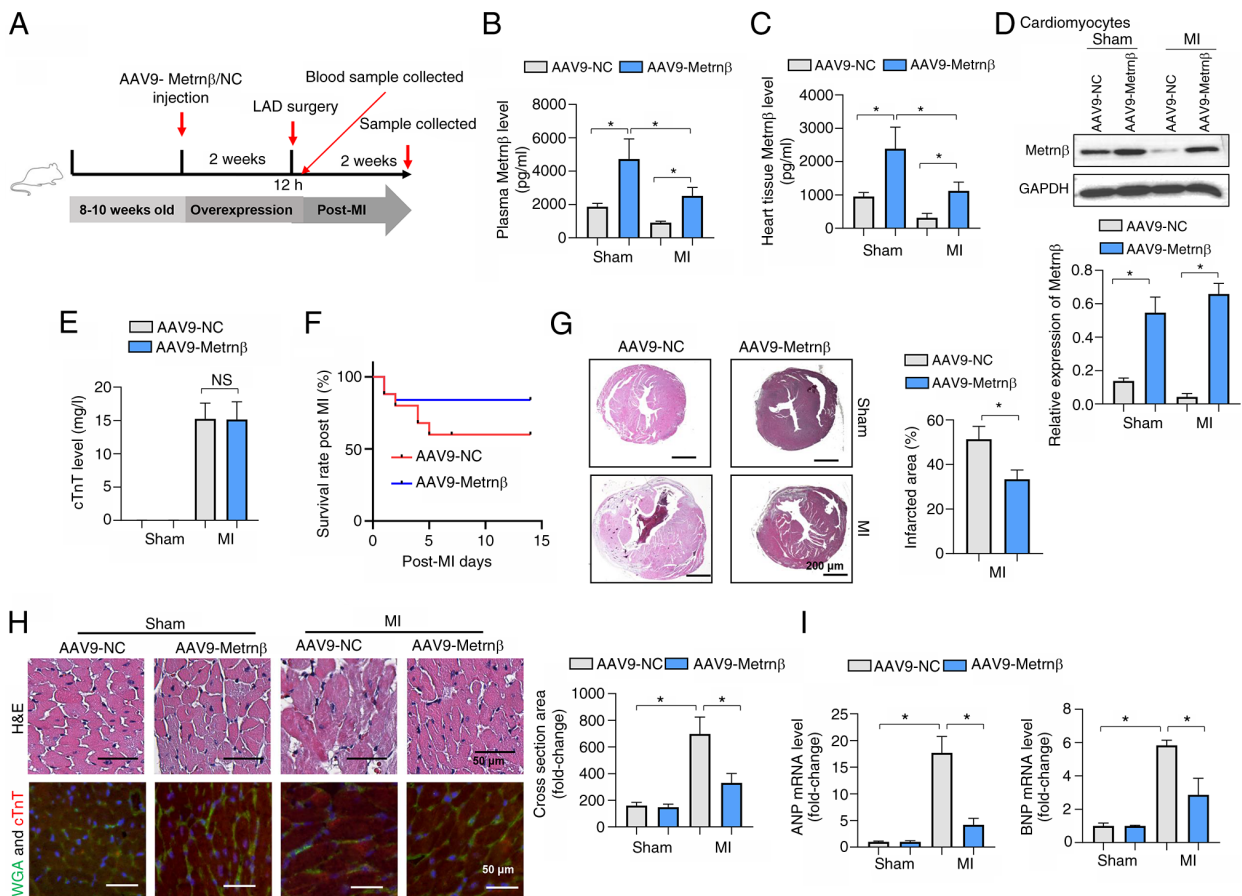
Figure 2. Metrnβ overexpression improves cardiac parameters post MI. (A) Animal experiment timeline. (B) Plasma levels of Metrnβ in mice after AAV9-Metrnβ or AAV9-NC injection (n=6). (C) Levels of Metrnβ in mouse hearts after AAV9-Metrnβ or AAV9-NC injection (n=6). (D) Levels of Metrnβ in cardiomyocytes isolated from adult mouse hearts (n=4). (E) Serum cTnT levels in MI mice 12 h post-LAD (n=6). (F) Survival rates of mice 2 weeks post-MI. (G) H&E staining and quantification of infarction size in mice (n=6). (H) H&E staining images, WGA and cTnT co-staining images, and quantified cross-sectional area in mice (n=6). (I) mRNA levels of ANP and BNP in mouse hearts (n=6). *P<0.05. Student's t-test was used for comparison between two groups. Two-way ANOVA was used for comparison among four groups with two variables: Treatment (AAV9-NC or AAV9-Metrnβ) and group (sham or MI). Metrnβ, meteorin-β; MI, myocardial infarction; NS, no significant difference; NC, negative control; LAD, left coronary artery ligation surgery; AAV9, adeno-associated virus 9; cTnT, cardiac troponin T; WGA, wheat germ agglutinin; ANP, atrial natriuretic peptide; BNP, B-type natriuretic peptide.
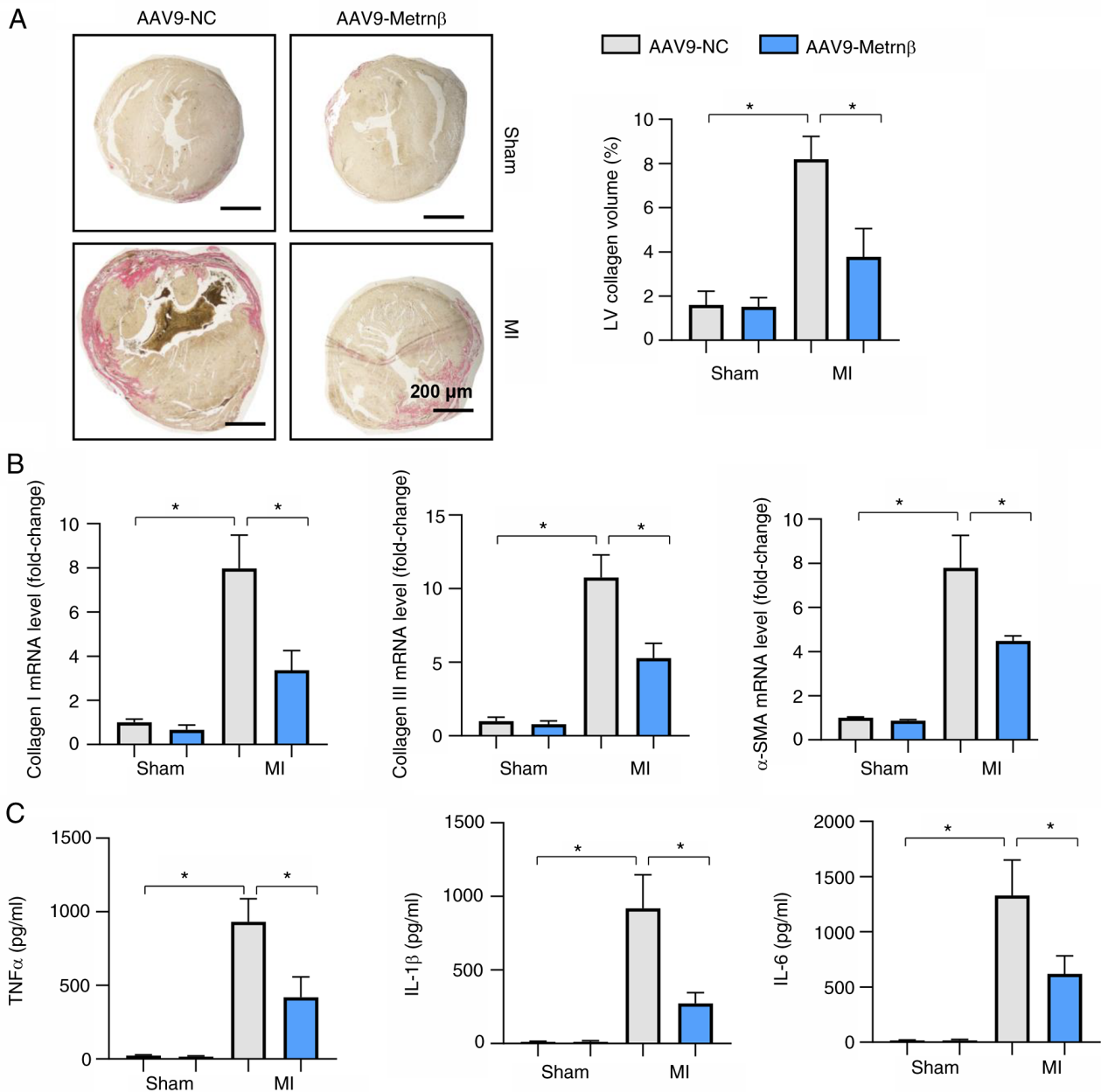
Figure 3. Metrnβ overexpression protects the heart from MI-induced fibrosis and inflammation. (A) Picrosirius red staining results and quantified results in mouse hearts (n=6). (B) mRNA levels of collagen I, collagen III and α-SMA in mouse hearts (n=6). (C) ELISA results of TNFα, IL-1β and IL-6 in mouse hearts (n=6). *P<0.05. Two-way ANOVA was used for comparison among four groups with two variables: Treatment (AAV9-NC or AAV9-Metrnβ) and group (sham or MI). Metrnβ, meteorin-β; MI, myocardial infarction; LV, left ventricular; α-SMA, α-smooth muscle actin; AAV9, adeno-associated virus 9; NC, negative control, TNFα, tumour necrosis factor α; IL, interleukin; ELISA, enzyme-linked immunosorbent assay.

and LV end systolic diameter (LVESD) were increased at 2 weeks after MI compared with those of the sham group (Fig. 4B-D). The LVEF and LVFS were decreased in the MI group compared with that of the sham group. Metrnβ overexpression improved cardiac dilation and function, as demonstrated by the reduced LVESD and increased LVEF and LVFS compared with the respective AAV9-NC groups. The pressure-volume measurement results also demonstrated that the LV pressure increase/delay at the end systolic phase (dp/dt max, dp/dt min) was reduced in the MI group compared with that in the sham group, but increased in the Metrnβ-overexpressing group compared with the AAV9-NC group (Fig. 4E; Table III).

Metrnβ overexpression protects against cardiomyocyte hypoxia injury. H9c2 cardiomyocytes were transfected with Ad-Metrnβ to overexpress Metrnβ. Ad-Metrnβ did not affect the cell viability under control or hypoxic conditions, as revealed using the CCK-8 assay (Fig. 5A). After 72 h of transfection, the levels of Metrnβ were increased in H9c2 cells in the Ad-Metrnβ group (Fig. 5A). Apoptosis was induced by 24 h of hypoxia, which was revealed by increased TUNEL-positive cells and caspase 3 activity. Metrnβ overexpression inhibited the apoptosis induced by hypoxia (Fig. 5B and C). Furthermore, the cell injury marker, LDH, was increased after 24 h of hypoxia in the hypoxia group. Cells treated with the Ad-Metrnβ exhibited reduced LDH levels compared with

Table III. Hemodynamic parameters in mice.

Parameter	AAV9-NC/Sham	AAV9-Metrnβ/Sham	AAV9-NC/MI	AAV9-Metrnβ/MI
HR (beats per min)	480.45±47.52	459.44±43.85	440.34±63.82	465.43±47.02
ESV (μl)	11.55±2.12	10.63±2.24	46.17±2.00[a]	24.03±2.87[b]
EDV (μl)	26.87±2.38	26.15±1.59	56.65±3.96[a]	36.60±2.53[b]
dp/dt max (mmHg/sec)	9,998.22±805.23	10,316.43±1,295.23	5,465.33±756.12[a]	7,988.67±1,127.33[a,b]
dp/dt min (mmHg/sec)	-10,366.44±1,212.34	-10,244.45±1,452.45	-5,270.22±894.34[a]	-7,251.34±659.34[b]
CO (μl/min)	7,389.33±419.45	7,148.54±125.56	4,536.22±312.09[a]	5,874.05±269.21[a,b]

[a]$P<0.05$ vs. the corresponding sham group. [b]$P<0.05$ vs. AAC9-NC/MI group. HR, heart rate; ESV, end systolic volume; EDV, end-diastolic volume; dp/dt max, maximal rate of pressure development; dp/dt min, maximal rate of pressure decay; CO, cardiac output; Metrnβ, Meteorin-β; MI, myocardial infarction; AAV9, adeno-associated virus 9; NC, negative control.

cells treated with the Ad-NC (Fig. 5D). Hypoxia also induced the release of proinflammatory cytokines (increased TNFα, IL-1β and IL-6 levels in the hypoxic group compared with the control group). The levels of these proinflammatory cytokines were reduced in the Ad-Metrnβ group compared with the Ad-NC group after exposure to hypoxic conditions (Fig. 5E).

To confirm the effect of Metrnβ on cardiomyocyte hypoxic injury, cells were transfected with Metrnβ siRNA to knockdown Metrnβ, and the decrease in the Metrnβ protein expression levels was confirmed after transfection (Fig. 5F). Metrnβ knockdown caused deteriorated hypoxia-induced cell injury and inflammation, as revealed by increased caspase 3 activity, LDH levels and pro-inflammatory cytokine levels compared with the siRNA NC (Fig. 5G-I).

Metrnβ inhibits autophagy in cardiomyocytes exposed to hypoxia. LC3 levels were increased in cells exposed to hypoxia (Fig. 6A). p62 levels were reduced in cells exposed to hypoxic conditions (Fig. 6C and D). Metrnβ overexpression reduced LC3 levels compared with the Ad-NC (Fig. 6A and B) and increased p62 protein levels under hypoxic conditions (Fig. 6C and D). However, the effects of Metrnβ overexpression on LC3 and p62 were not significantly inhibited by the classic autophagy inhibitor BAF, which works by blocking the autophagosome lysosomal fusion (Fig. 6A-D). Cells were transfected with Ad-mRFP-GFP-LC3, which served as a dual-fluorescence pH sensor for autophagic vacuoles and revealed autolysosome formation. mRFP-stained LC3 (indicating the formation of autophagosomes) and GFP-LC3 (representing the remaining autophagosomes after degradation) were both revealed to increase with hypoxic stimuli but were reduced by Metrnβ overexpression (Fig. 6B). However, the degradation rate (red-green puncta/red puncta) was unaltered when Metrnβ was overexpressed under both physiological and hypoxic conditions (Fig. 6B). Furthermore, LC3II levels were also increased, and p62 levels were reduced in MI heart tissue. Metrnβ overexpression reduced LC3 levels and increased p62 protein levels under hypoxic conditions when compared with the Ad-NC (Fig. 6C). Furthermore, Metrnβ overexpression reduced LC3 levels and increased p62 protein levels in MI heart tissue when compared with the Ad-NC (Fig. 6D). Taken together, the data demonstrated that the protection induced by Metrnβ was not due to the

regulation of autophagosome degradation, but through the effect on autophagy induction.

Autophagy activation counteracts the protective effects of Metrnβ. To confirm the effect of Metrnβ on autophagy, an autophagy activator, rapamycin, was used. Rapamycin increased hypoxia-induced apoptosis as revealed by the increased number of TUNEL-positive cells, increased caspase 3 activity and increased LDH levels (Fig. 7A-C). Rapamycin also exacerbated hypoxia-induced cell inflammation, as revealed by increased levels of proinflammatory factors (Fig. 7D). Metrnβ overexpression could not reverse the rapamycin-induced effects on the cardiomyocytes (Fig. 7A-D). These data indicate that autophagy activation could abolish the protective effects of Metrnβ on cardiomyocytes.

Discussion

In the present study, the expression levels of Metrnβ were first revealed to be reduced after MI both in plasma as well as in heart tissues, which was localized to the cardiomyocytes. The effect of Metrnβ on cardiac remodelling after MI was then evaluated and it was revealed that Metrnβ could reduce the infarct size and improve survival rates and cardiac function at 2 weeks post-MI. The present study also revealed that Metrnβ suppressed cardiac hypertrophy, fibrosis and inflammation by inhibiting autophagy induction but not the autophagosome degradation after MI. Autophagy activation abolished the protective effects of Metrnβ on cardiomyocytes under hypoxic conditions. Therefore, Metrnβ may become a new therapeutic target for inhibiting the progression of heart failure after MI.

MI places a significant burden on global health, affecting >7 million individuals worldwide each year (3). In the past 10 years, early revascularization has had far-reaching significance for the treatment of MI (1). The 30-day survival rate of acute ST segment elevation MI has increased to 95% (4). However, despite revascularization, patients with AMI have a 75% probability of developing heart failure within 5 years (2,3). An increasing number of patients that survive AMI develop heart failure. Therefore, it is important to prevent or even reverse heart failure after MI and to develop novel treatments focusing on the prevention of heart failure. Metrnβ is a secretory protein involved in glucose metabolism (8). A

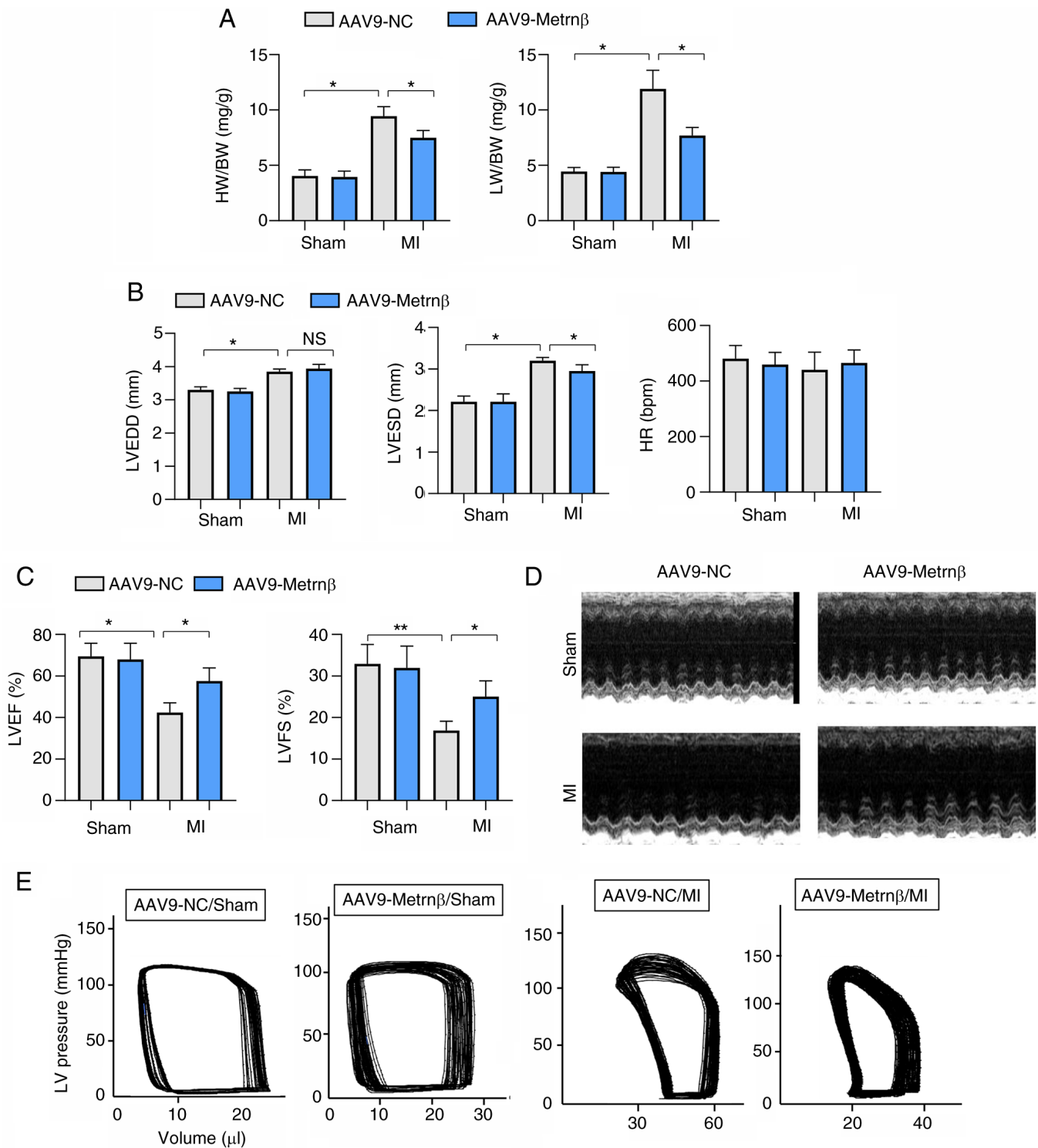Figure 4. Metrnβ overexpression preserves cardiac function post MI. (A) HW/BW and LW/BW in mouse hearts (n=8). (B) Echocardiography results of LVEDD, LVESD and HR in mouse hearts (n=6). (C) Echocardiography results of LVEF and LVFS in mouse hearts (n=6). (D) Echocardiography results in mouse hearts (n=6). (E) Representative images of pressure-volume measurements in mouse hearts (n=6). $^*P<0.05$ and $^{**}P<0.01$. Two-way ANOVA was used for comparison among four groups with two variables: Treatment (AAV9-NC or AAV9-Metrnβ) and group (sham or MI). Metrnβ, meteorin-β; MI, myocardial infarction; HW, heart weight; BW, body weight; LW, lung weight; LV, left ventricular; LVEDD, LV end diastolic diameter; LVESD, LV end systolic diameter; HR, heart rate; LVEF, LV ejection fraction; LVFS, LV fractional shortening; AAV9, adeno-associated virus 9; NC, negative control; NS, no significant difference.

previous study revealed that a decrease in plasma Metrnβ was associated with insulin resistance in patients with type 2 diabetes (10). Metrnβ was also reported to inhibit airway inflammation in house dust mite-induced allergic asthma (24). Ushach et al (10) reported that Metrnβ regulated inflammatory

responses in macrophages. It was also revealed that Metrnβ knockout mice exhibited increased cytokine production. Recently, Rupérez et al (11) revealed that Metrnβ ameliorated cardiac dysfunction and cardiac hypertrophy in response to isoproterenol and ageing. Hu et al (25) recently reported that

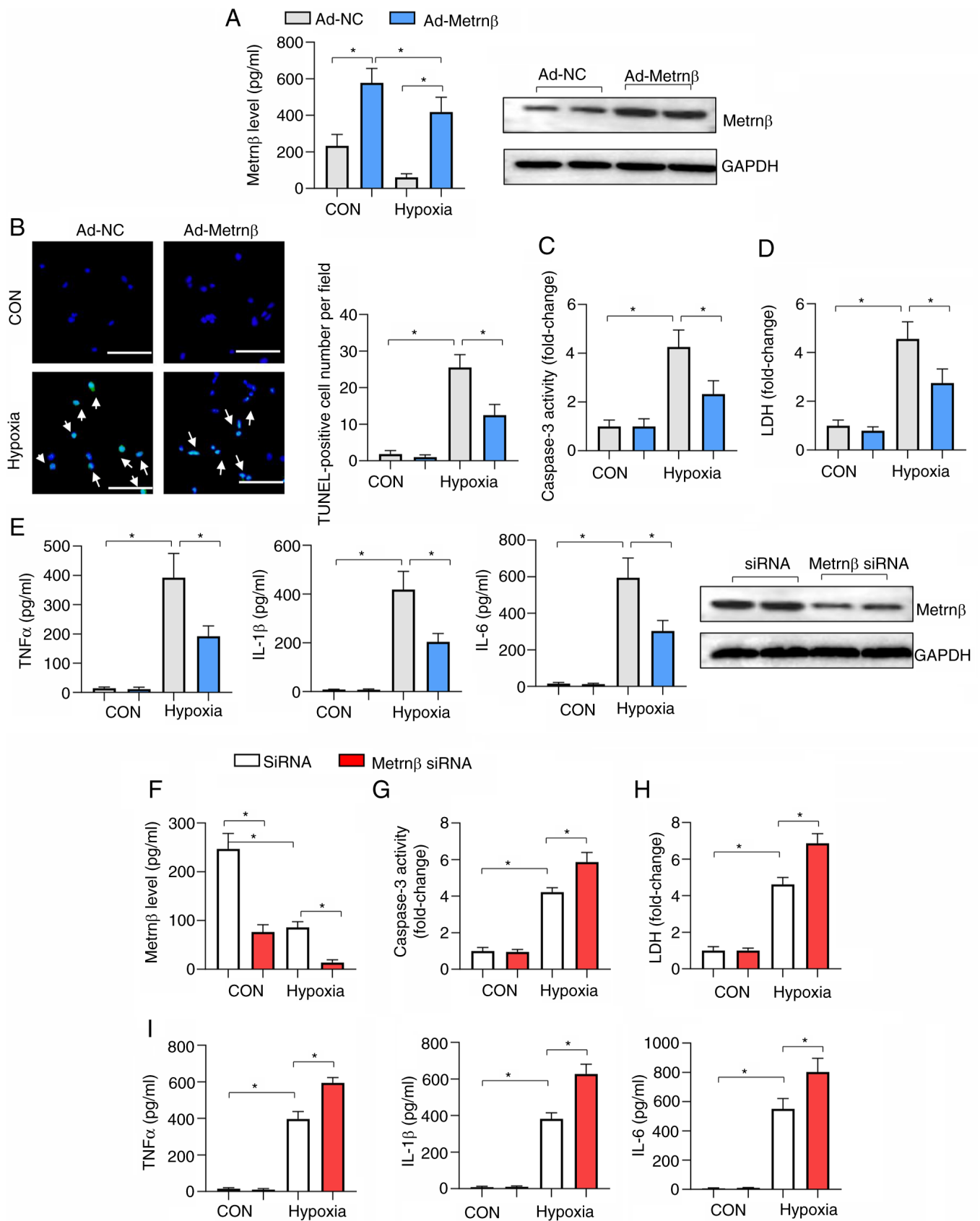Figure 5. Metrnβ overexpression protects against cardiomyocyte hypoxia injury. (A-E) Cells were transfected with Ad-Metrnβ. (A) Protein levels of Metrnβ and cell viability in cardiomyocytes (n=6). (B) TUNEL staining and quantified results in cardiomyocytes (n=6; scale bar, 100 μm). (C) caspase 3 activity and (D) LDH levels in cardiomyocytes (n=6). (E) ELISA results of TNFα, IL-1β and IL-6 in cardiomyocytes (n=6). (F-I) Cells were transfected with Metrnβ siRNA. (F) Protein levels of Metrnβ in cardiomyocytes transfected with Metrnβ siRNA or scRNA (n=6). (G) caspase 3 activity and (H) LDH level in cardiomyocytes (n=6). (I) ELISA results of TNFα, IL-1β and IL-6 in cardiomyocytes (n=6). $^{*}P<0.05$. Two-way ANOVA was used for comparison among four groups with two variables: Treatment (Ad-NC or Ad-Metrnβ) and group (CON or hypoxia). Metrnβ, meteorin-β; Ad, adenovirus; LDH, lactate dehydrogenase; TNFα, tumour necrosis factor α; IL, interleukin; siRNA, small interfering RNA; NC, negative control; CON, control; scRNA, scrambled RNA.
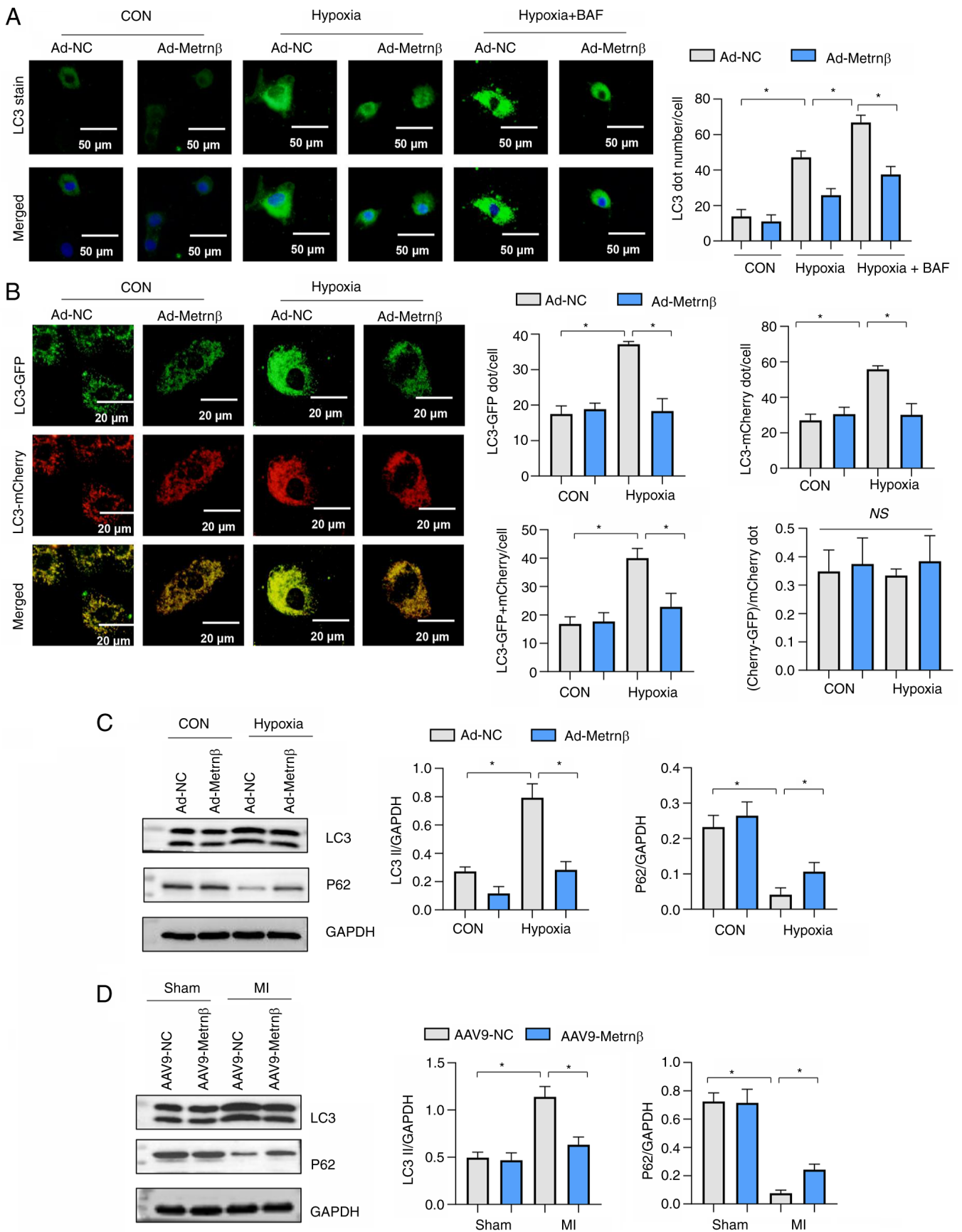
Figure 6. Metrnβ inhibits autophagy in cardiomyocytes exposed to hypoxia. (A) LC3 staining and quantified results in cardiomyocytes (n=6). (B) Autophagic flux analysis and quantified results in cardiomyocytes (n=6). (C) LC3 and p62 protein levels in cardiomyocytes (n=6). (D) LC3 and P62 protein levels in mouse hearts (n=6). *P<0.05. Two-way ANOVA was used for comparison among groups with two variables: Treatment (Ad-NC or Ad-Metrnβ/AAV9-NC or AAV9-Metrnβ) and group (CON or hypoxia or hypoxia plus BAF). Metrnβ, meteorin-β; MI, myocardial infarction; Ad, adenovirus; AAV9, adeno-associated virus 9; NC, negative control; NS, no significant difference; CON, control; BAF, bafilomycin A1; GFP, green fluorescent protein.
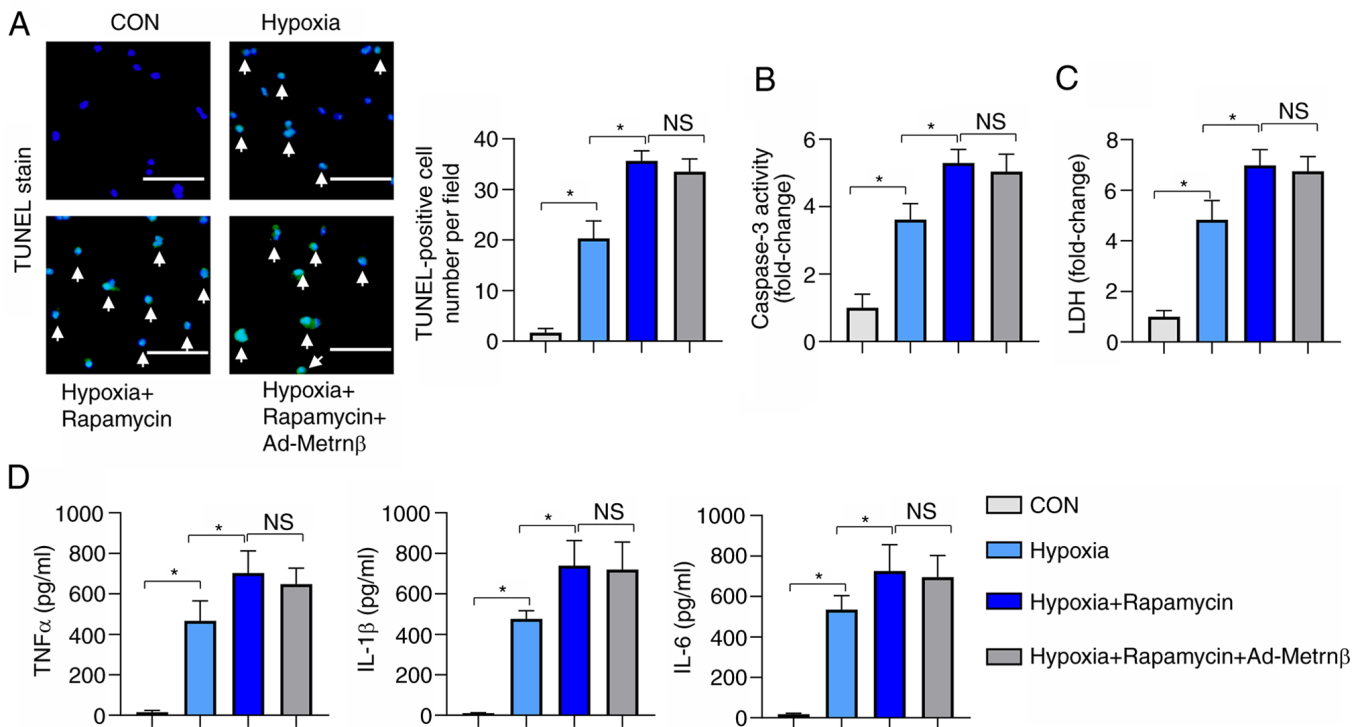
Figure 7. Autophagy activation counteracts the protective effects of Metrnβ. H9c2 cells were treated with rapamycin and transfected with Ad-Metrnβ. (A) TUNEL staining and quantified results in cardiomyocytes exposed to hypoxia (n=6; scale bar, 100 μm). (B) caspase 3 activity and (C) LDH levels in cardiomyocytes exposed to hypoxia (n=6). (D) ELISA results of TNFα, IL-1β and IL-6 in cardiomyocytes exposed to hypoxia (n=6). *P<0.05. One-way ANOVA analysis followed by Tukey's post hoc test was used for comparison among the four groups. Metrnβ, meteorin-β; Ad, adenovirus; CON, control; TNFα, tumour necrosis factor α; IL, interleukin; LDH, lactate dehydrogenase; NS, no significant difference; ELISA, enzyme-linked immunosorbent assay.

by modulating the cAMP/protein kinase A/Sirtuin 1 pathway, Metrnβ protein inhibited doxorubicin-induced cardiotoxicity. In the present study, the data demonstrated that Metrnβ expression levels were reduced after MI. Furthermore, the present study revealed that Metrnβ overexpression using AAV9-Metrnβ delivery could offer cardiac protection to hearts subjected to MI, which was indicated by the reduced cardiac infarct size, improved cardiac function, and reduced cardiac hypertrophy, fibrosis and inflammatory response 2 weeks after MI. Since it was revealed that the decrease in the Metrnβ protein levels was localized in cardiomyocytes and not in the macrophage cells in mice heart tissues, the *ex vivo* cardiomyocyte model was used to further explore whether Metrnβ could protect the cardiomyocytes from hypoxic damage. The present study revealed that Metrnβ overexpression in cardiomyocytes reduced hypoxia-induced apoptosis and inflammation. Thus, the results suggest that Metrnβ could directly affect cardiomyocytes to exert protective effects.

Autophagy is another type of cell death. Intracellular components (including proteins and organelles) are digested and recovered through lysosomal degradation to maintain energy production and protein synthesis to promote cell survival (26). Autophagy under stress, especially during ischaemia, starvation and β-adrenaline stimulation, allows myocardial cells to remove damaged or misfolded proteins, organelles and aggregates (27). Normally, autophagy can remove damaged cells and organelles, whereas abnormal autophagy leads to abnormal protein accumulation, which can lead to heart failure due to a variety of causes (such as hypertension and myocardial infarction) (7,28). Autophagy

was previously revealed to be upregulated in cardiomyocytes in heart failure (6). In addition, impaired autophagy serves a pathological role in the progression of heart failure (7,28). In the present study, augmented autophagy activation in hypoxic cardiomyocytes and MI heart tissues was also revealed. It has been reported that Metrnβ ameliorates diabetic cardiomyopathy via the inactivation of cGAS/STING signalling, which is dependent on LKB1/AMPK/ULK1-mediated autophagy (27). Therefore, the present study hypothesized that autophagy regulation may serve a role in the protection of Metrnβ against MI injury. It was revealed in the present study that Metrnβ inhibited the increase in the autophagy of cardiomyocytes in hypoxic conditions. With the administration of BAF, an autophagosome degradation inhibitor, it was confirmed that Metrnβ inhibited autophagy induction without affecting autophagosome degradation. mTOR kinases are associated with protein synthesis and autophagy, and mTORC1 inhibits catabolic processes, including autophagy. Rapamycin is an allosteric inhibitor of mTORC1, which activates autophagy (27). To test this relationship, rapamycin in cardiomyocytes under hypoxic conditions was used to activate autophagy, and aggravated cell injury was revealed upon hypoxia. Furthermore, the protective effects of Metrnβ were abolished, which confirmed that the cardiac protection of Metrnβ was dependent on autophagy inhibition in MI.

In summary, Metrnβ suppresses cardiac hypertrophy, fibrosis and inflammation after MI together with reduced autophagy. Autophagy activation abolished the protective effects of Metrnβ on cardiomyocytes under hypoxic

conditions. Metrnβ may be a novel therapeutic target for inhibiting the progression of heart failure after MI by inhibiting autophagy.

Acknowledgements

Not applicable.

Availability of data and materials

The datasets used and/or analysed during the current study are available from the corresponding author on reasonable request.

Authors' contributions

JS and LL contributed to the conception of the study and the design of the experiments. JS, GL and LX performed the experiments. WZ and XZ analysed the experimental results and revised the manuscript. JS and LL wrote and revised the manuscript. JS and LL confirm the authenticity of all the raw data. All authors read and approved the final version of the manuscript.

Ethics approval and consent to participate

The animal experiments were performed according to the Animal Research: Reporting of *in vivo* Experiments guidelines and were approved by the Animal Care and Use Committee of the First Affiliated Hospital of Zhengzhou University (approval no. 2021-02623).

Patient consent for publication

Not applicable.

Competing interests

The authors declare that they have no competing interests.

References

1. Bahit MC, Kochar A and Granger CB: Post-myocardial infarction heart failure. JACC Heart Fail 6: 179-186, 2018.
2. Berezin AE and Berezin AA: Adverse cardiac remodelling after acute myocardial infarction: Old and new biomarkers. Dis Markers 2020: 1215802, 2020.
3. Jenča D, Melenovský V, Stehlik J, Staněk V, Kettner J, Kautzner J, Adámková V and Wohlfahrt P: Heart failure after myocardial infarction: Incidence and predictors. ESC Heart Fail 8: 222-237, 2021.
4. Mouton AJ, Rivera OJ and Lindsey ML: Myocardial infarction remodeling that progresses to heart failure: A signaling misunderstanding. Am J Physiol Heart Circ Physiol 315: H71-H79, 2018.
5. Du J, Liu Y and Fu J: Autophagy and heart failure. Adv Exp Med Biol 1207: 223-227, 2020.
6. Du J, Li Y and Zhao W: Autophagy and myocardial ischemia. Adv Exp Med Biol 1207: 217-222, 2020.
7. Liu CY, Zhang YH, Li RB, Zhou LY, An T, Zhang RC, Zhai M, Huang Y, Yan KW, Dong YH, et al: LncRNA CAIF inhibits autophagy and attenuates myocardial infarction by blocking p53-mediated myocardin transcription. Nat Commun 9: 29, 2018.
8. Baht GS, Bareja A, Lee DE, Rao RR, Huang R, Huebner JL, Bartlett DB, Hart CR, Gibson JR, Lanza IR, et al: Meteorin-like facilitates skeletal muscle repair through a Stat3/IGF-1 mechanism. Nat Metab 2: 278-289, 2020.
9. Wu Q, Dan YL, He YS, Xiang K, Hu YQ, Zhao CN, Zhong X, Wang DG and Pan HF: Circulating meteorin-like levels in patients with type 2 diabetes mellitus: A meta-analysis. Curr Pharm Des 26: 5732-5738, 2020.
10. Ushach I, Arrevillaga-Boni G, Heller GN, Pone E, Hernandez-Ruiz M, Catalan-Dibene J, Hevezi P and Zlotnik A: Meteorin-like/Meteorin-β is a novel immunoregulatory cytokine associated with inflammation. J Immunol 201: 3669-3676, 2018.
11. Rupérez C, Ferrer-Curriu G, Cervera-Barea A, Florit L, Guitart-Mampel M, Garrabou G, Zamora M, Crispi F, Fernandez-Solà J, Lupón J, et al: Meteorin-like/Meteorin-β protects heart against cardiac dysfunction. J Exp Med 218: e20201206, 2021.
12. Cai J, Wang QM, Li JW, Xu F, Bu YL, Wang M, Lu X and Gao W: Serum meteorin-like is associated with weight loss in the elderly patients with chronic heart failure. J Cachexia Sarcopenia Muscle 13: 409-417, 2022.
13. Li F, Zong J, Zhang H, Zhang P, Xu L, Liang K, Yang L, Yong H and Qian W: Orientin reduces myocardial infarction size via eNOS/NO signaling and thus mitigates adverse cardiac remodeling. Front Pharmacol 8: 926, 2017.
14. Livak KJ and Schmittgen TD: Analysis of relative gene expression data using real-time quantitative PCR and the 2(-Delta Delta C(T)) method. Methods 25: 402-408, 2001.
15. Wu QQ, Xiao Y, Duan MX, Yuan Y, Jiang XH, Yang Z, Liao HH, Deng W and Tang QZ: Aucubin protects against pressure overload-induced cardiac remodelling via the beta₃-adrenoceptor-neuronal NOS cascades. Br J Pharmacol 175: 1548-1566, 2018.
16. Xiao Y, Yang Z, Wu QQ, Jiang XH, Yuan Y, Chang W, Bian ZY, Zhu JX and Tang QZ: Cucurbitacin B protects against pressure overload induced cardiac hypertrophy. J Cell Biochem 118: 3899-3910, 2017.
17. Franke WW, Dörflinger Y, Kuhn C, Zimbelmann R, Winter-Simanowski S, Frey N and Heid H: Protein LUMA is a cytoplasmic plaque constituent of various epithelial adherens junctions and composite junctions of myocardial intercalated disks: A unifying finding for cell biology and cardiology. Cell Tissue Res 357: 159-172, 2014.
18. Guo Z, Tuo H, Tang N, Liu FY, Ma SQ, An P, Yang D, Wang MY, Fan D, Yang Z and Tang QZ: Neuraminidase 1 deficiency attenuates cardiac dysfunction, oxidative stress, fibrosis, inflammatory via AMPK-SIRT3 pathway in diabetic cardiomyopathy mice. Int J Biol Sci 18: 826-840, 2022.
19. Wan N, Liu X, Zhang XJ, Zhao Y, Hu G, Wan F, Zhang R, Zhu X, Xia H and Li H: Toll-interacting protein contributes to mortality following myocardial infarction through promoting inflammation and apoptosis. Br J Pharmacol 172: 3383-3396, 2015.
20. Wu QQ, Xu M, Yuan Y, Li FF, Yang Z, Liu Y, Zhou MQ, Bian ZY, Deng W, Gao L, et al: Cathepsin B deficiency attenuates cardiac remodeling in response to pressure overload via TNF-α/ASK1/JNK pathway. Am J Physiol Heart Circ Physiol 308: H1143-H1154, 2015.
21. Fan D, Yang Z, Yuan Y, Wu QQ, Xu M, Jin YG and Tang QZ: Sesamin prevents apoptosis and inflammation after experimental myocardial infarction by JNK and NF-κB pathways. Food Funct 8: 2875-2885, 2017.
22. Lomas O, Brescia M, Carnicer R, Monterisi S, Surdo NC and Zaccolo M: Adenoviral transduction of FRET-based biosensors for cAMP in primary adult mouse cardiomyocytes. Methods Mol Biol 1294: 103-115, 2015.
23. Alonso-Herranz L, Porcuna J and Ricote M: Isolation and purification of tissue resident macrophages for the analysis of nuclear receptor activity. Methods Mol Biol 1951: 59-73, 2019.

24. Gao X, Leung TF, Wong GW, Ko WH, Cai M, He EJ, Chu IM, Tsang MS, Chan BC, Ling J, *et al*: Meteorin-β/Meteorin like/IL-41 attenuates airway inflammation in house dust mite-induced allergic asthma. Cell Mol Immunol 19: 245-259, 2022.
25. Hu C, Zhang X, Song P, Yuan YP, Kong CY, Wu HM, Xu SC, Ma ZG and Tang QZ: Meteorin-like protein attenuates doxorubicin-induced cardiotoxicity via activating cAMP/PKA/SIRT1 pathway. Redox Biol 37: 101747, 2020.
26. Wang D, Lv L, Xu Y, Jiang K, Chen F, Qian J, Chen M, Liu G and Xiang Y: Cardioprotection of panax notoginseng saponins against acute myocardial infarction and heart failure through inducing autophagy. Biomed Pharmacother 136: 111287, 2021.
27. Gao G, Chen W, Yan M, Liu J, Luo H, Wang C and Yang P: Rapamycin regulates the balance between cardiomyocyte apoptosis and autophagy in chronic heart failure by inhibiting mTOR signaling. Int J Mol Med 45: 195-209, 2020.
28. Fei Q, Ma H, Zou J, Wang W, Zhu L, Deng H, Meng M, Tan S, Zhang H, Xiao X, *et al*: Metformin protects against ischaemic myocardial injury by alleviating autophagy-ROS-NLRP3-mediated inflammatory response in macrophages. J Mol Cell Cardiol 145: 1-13, 2020.